The Effect of Source Separation on the Waste Disposal Process: Case Study in Hangzhou

Yuyang Long and Dongsheng Shen

Abstract MSW source separation is a key procedure for its later processing. Kitchen waste, the main contributor to moisture content, accounts for a very high proportion (~60%) in MSW composition. The feasible way to dispose of MSW before or after separation depends on the reasonable disposal of kitchen waste. Here, a case study from Hangzhou, China, is presented in terms of the source separation effect on the waste disposal process. In Hangzhou, three strategies, including direct digestion without separation, composting after separation, and co-digestion with fruit and vegetable waste, were explored. It indicates that:

1. MSW digestion without separation is a possible means of refuse disposal. The refuse and leachate in the reactor connected with the aged refuse column and reached a strongly degraded and more stable state compared with directly recycled leachate.
2. Kitchen waste composting after source separation is a better choice. However, the high water content is the key issue that needs attention. Especially, the water state should be paid more attention to. Additives like PAM can significantly enhance the capillary force and delay the decrease in moisture content during aerobic decomposition and improve the composting process.
3. Kitchen waste co-digestion with fruit and vegetable waste has a high application potential. The two-phase AD with 50% kitchen waste was a reasonable ratio in this two-phase AD system.

Keywords Co-digestion, Composting, Digestion, Kitchen waste

Y. Long and D. Shen (✉)
Zhejiang Provincial Key Laboratory of Solid Waste Treatment and Recycling, School of Environmental Science and Engineering, Zhejiang Gongshang University, Hangzhou 310012, China
e-mail: longyy@zjgsu.edu.cn; shends@zju.edu.cn

R. Maletz et al. (eds.), *Source Separation and Recycling*,
Hdb Env Chem (2018) 63: 199–226, DOI 10.1007/698_2017_31,

Contents

Abbreviations

AD	Anaerobic digestion
APR	Acidogenic phase reactor
COD	Chemical oxygen demand
CW	The water removed at 60 and 70°C
EC	Electrical conductivity
EW	The water removed at 30, 40, and 50°C
FVW	Fruit–vegetable waste
HRT	Hydraulic retention time
KW	Kitchen waste
MMLW	The water removed at 80, 90, 100, and 105°C
MPR	Methanogenic phase reactor
MSW	Municipal solid waste
NDF	Neutral detergent fiber
NDS	Neutral detergent solute
PAM	Polyacrylamide
TN	Total nitrogen
TS	Total solids
VFA	Volatile fatty acids
VRR	Volume reduction rate
VS	Volatile solid
WHCs	Water holding capacities

1 Introduction

MSW relates to a broad array of issues, such as social, economic, environmental, technological, and legislative and is regarded as unwanted materials to be disposed of. Currently, the world generates approximately 1.3 billion tons of MSW per year, which is expected to increase to 2.2 billion tons by 2025 [1]. Waste separation at the source is subjectively done by individuals collecting recyclable or compostable materials from commingled waste and placing it at disposal locations at their homes for collection. The main purposes of source separation are recycling, reuse, and

reducing environmental as well as economic burdens to the MSW management systems. The major impact on the effectiveness of MSW management systems comes from the separation of waste causing essential changes in the quantity and quality of waste reaching the final management process, or waste treatment and disposal [1].

Hangzhou, located along the southeastern coast of China, is the capital of Zhejiang Province. The total area of the city covers 16,596 km^2 with a population of 8,892,000. It is a key central city in the Yangtze River Delta and a traffic hub in southeastern China. Hangzhou is in a subtropical zone with a monsoon climate. The annual MSW output of Hangzhou was 3.65 million tons in 2015. From the MSW source separation guidelines in Hangzhou, MSW must be separated into at least four fractions. The Department of Urban Appearance and Environmental Renovation guides the MW classification based on the principle of easy reduction, recycling, identification, and classification. The standard of classification of MSW in rural areas could be appropriately adjusted to combine with the actual local situation (Fig. 1).

1. Recoverable matter is a component of unpolluted MSW suitable for recycling and reutilization, such as paper, plastic, glass and metal, etc.
2. Hazardous waste is a component of MSW, which can cause direct or potential hazards to human health or the environment. This includes waste rechargeable batteries, waste button cells, waste fluorescent lamps, waste medicines, waste pesticides, waste paint, daily chemical waste, waste mercury products, etc.
3. Food waste, which is produced during the process of production by restaurant operators, unit dining rooms, etc. This also includes food waste from families' everyday life and putrescible wastes from the market, as they all belong to the refuse.

Fig. 1 MSW source separation categories in Hangzhou

4. Other wastes not allocated to fractions for recoverable substances include hazardous waste and food waste. These are mixed, soiled, and difficult to classify, in contrast to paper, plastics, glass, metals, fabrics and wood, etc.

2 The Effect of Source Separation on Waste Disposal Processing

Kitchen waste accounts for a very high proportion (~60%) of MSW composition in Hangzhou. Moreover, it is also the main contributor to the moisture content. Therefore, the feasible way to dispose of MSW before or after separation depends on the reasonable disposal of kitchen waste. Three strategies, including direct digestion without separation, composting after separation, and co-digestion with fruit and vegetable waste, were explored. Here, the main processes and results are presented.

2.1 MSW Digestion Without Separation

2.1.1 Research Setup

For this processing, the results of pilot scale research are shown. Two digestion systems were designed and operated (Fig. 2), namely, system I and system II. System I comprised only waste column R1 loaded with fresh refuse, from which the leachate was collected by tank J1, and then directly recycled using a pump for nearly 16 h every week. System II was a sequencing batch reactor, which was comprised of waste column R2 loaded with fresh refuse and R3 loaded with 1 year of aged refuse. The leachate generated from columns R2 and R3 was first drained into recirculation tanks J2 and J3, respectively, and in the meantime, R2 and R3 were fed with the leachate from tanks J3 and J2, respectively, by pump for nearly 16 h every week. Three waste columns were constructed with the same size and materials with a thickness of 5 cm, an internal diameter of 1,400 mm, and a height of 2,000 mm. All of the reactors were placed in an outdoor venue of Hangzhou and operated for 20 weeks during the experiment.

2.1.2 MSW Composition and Operation

The MSW used was not separated. Columns R1 and R2 were packed with 1,600 kg of fresh refuse collected from Hangzhou at a wet density of 700 kg m^{-3}, respectively, and the average composition was (by wet weight, w/w) 63.12% kitchen residue, 12.81% slag, 8.93% paper, 2.54% glass, 8.38% plastics, 0.11% metal, 1.15% cellulose textile, 1.95% stone and brick, and 1.01% other. The initial

Fig. 2 Setup of tested systems

characteristics of the fresh refuse were 710 mg kg^{-1} TN (dry refuse), 62.72% VS (w/w), 50.97% biodegradable matter (w/w), 6.98 pH, and 60.73% moisture content.

2.1.3 Results

Settlement of Refuse in Three Waste Columns

VRR data for the refuse of reactors R1, R2, and R3 are presented in Fig. 3a. As illustrated, the settlement of refuse in the three columns mainly took place in the first 20 days. The VRR showed a similar trend in two fresh refuse columns, columns R1 and R2, both of which increased linearly up to 20% after the experiment had been started for 2 days, then their VRR increased slowly with different rates, and column R2 connected with aged refuse column R3 and showed a more rapid rate than column R1, though both of them maintained approximately 50% and 44% after 40 days, respectively. No significant change in VRR was detected in the old waste column, R3. Only a small increase in VRR was observed, which stagnated at 7% after 7 days. This indicates a substantial stabilization of the decline in R3.

Characteristics of Leachate VFA and pH

VFA are the most important intermediates in the anaerobic digestion process, and there is a close relationship between VFA concentration and pH value. Therefore,

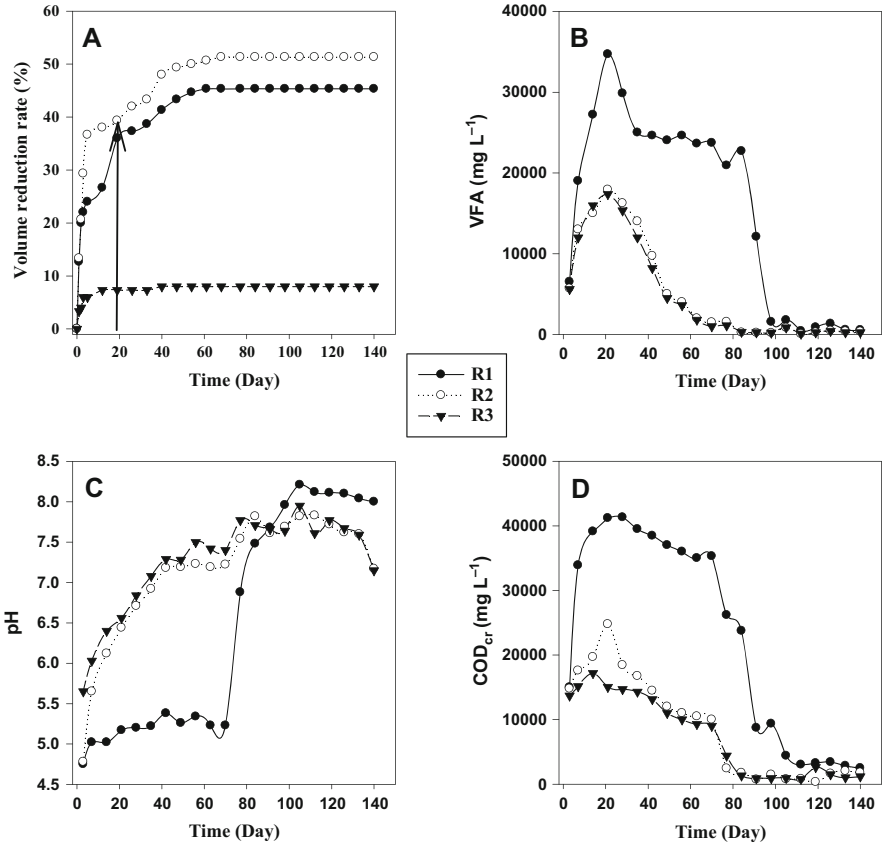

Fig. 3 Time evolutions of VVR (**a**) for refuse, VFA (**b**), pH (**c**) and COD (**d**) in leachate during operation

VFA have been monitored for a long time as process performance indicators [2]. As can be seen from Fig. 3b, the VFA concentration presented the same trend in the leachate from reactors R2 and R3, both of which increased slowly at the beginning of the 21 days, and reached maximum values of 17,932 and 17,369 mg L^{-1}, respectively. Then from day 28, the leachate concentration of VFA began to decrease slowly and finally maintained around 350 and 250 mg L^{-1}, respectively. However, the leachate VFA concentrations increased linearly at the beginning of 21 days for reactor R1 and reached maximum value of 34,680 mg L^{-1} on day 21, which is nearly two times higher than the leachate VFA concentration of reactor R2. From then on, the VFA concentration presented a different trend. It first decreased to 25,000 mg L^{-1} on day 35, and then no considerable change was observed during the succeeding 49 days. Afterwards, the leachate VFA concentration for reactor R2 decreased rapidly and was finally maintained at approximately 550 mg L^{-1}. The rapid increase of VFA in landfill reactors R1 and R2 was

attributed to the accumulation of soluble long-chain fatty acids in the leachate. As known to all, acidogens are fast-growing bacteria with a minimum doubling time of around 30 min, and then most of the soluble organic refuse was converted to VFA in a short time interval. As a result, the leachate VFA concentration reached its peak value within 21 days. However, reactor R2 was connected with aged refuse reactor R3, and the VFA produced by reactor R2 was neutralized by the leachate from the aged refuse reactor, which showed the advantage of the two-phase processes for higher bioconversion efficiency and system stability compared to the directly recirculated reactor. Therefore, although reactors R1 and R2 were loaded with the same refuse, the peak and average value or time span of the high concentration of VFA in reactor R2 was lower or shorter than that in reactor R1.

The pH values were in accordance with the concentration of VFA monitored for all three reactors. Leachate pH values of reactors R2 and R3 increased after the experiment started and reached 7.18 and 7.29 on day 42, respectively, and then stayed within the range of 7.19–8.04 in the succeeding 98 days, indicating that reactor R2 had already transferred from the acid phase to the methane fermentation phase. On the contrary, an ensiling problem was observed in landfill reactor R1, no considerable variation was observed in the leachate from this reactor, and the pH values remained in the range of 4.75–5.38 in the first 10 weeks due to the accumulation of VFA (Fig. 3c). After day 70, the leachate pH values began to increase and reached 8 after day 105 in reactor R1. After that, no significant variation was observed and was measured between 7.78 and 8.21. Low pH values observed at the early stage in reactor R1 may be ascribed to the production of low alkalinity in reactor R1, which is not enough for maintaining the neutral pH and buffering the VFA produced [3, 4]. The sudden increase on day 77 for reactor R1 might have resulted from the hydrolyzing and fermentation of VFA to carbon dioxide and methane, which agreed with the decrease in the leachate VFA concentration. These results indicated that the fresh refuse reactor connected with the aged refuse column was beneficial to reaching a strongly degraded and more stable state compared with directly recycled leachate.

Characteristics of Leachate COD

As was shown in Fig. 3d, due to the rapid release and hydrolysis of polymers such as carbohydrates, fats, and proteins from the fresh refuse into the leachate, COD concentrations increased from 15,000 and 14,800 mg $L^{-1}$to maximum values of 41,184 and 24,770 mg L^{-1} for reactors R1 and R2 after 21 days of operation, respectively. After reaching maximum values, the leachate COD concentrations for reactor R2 decreased slowly and maintained at 10,000 mg L^{-1} on day 70. Afterwards, the concentration began to decrease rapidly and maintained around 1,778 mg L^{-1}. However, no significant change was observed in the leachate COD concentrations for reactor R1 from days 22 to 70, which is in accordance with the progression law of VFA and low pH value attained from the former elucidation. Thus, the long stage for a high level of COD from reactor R1 might be attributed to

the low activity of methanogenic bacteria, which only grow within a narrow pH range around neutrality [5]. Afterwards, with the decrease of VFA concentration and increase in pH value, COD concentrations began to decrease rapidly for reactor R1, and the concentration on days 91–140 were determined to be 8,720–2,500 mg L^{-1}. As for reactor R3, the leachate COD concentrations increased slightly during the first 2 weeks, and then decreased gradually to 9,000 mg L^{-1}. Afterwards, the concentration began to decrease rapidly and maintained at around 1,185 mg L^{-1}. Therefore, the combination with an aged refuse reactor not only had a beneficial effect on the stabilization of fresh refuse but also on the degradation of leachate organic constituents, such as VFA and COD. The main reason for that might be the high microbial ability in aged refuse.

Characteristics of Leachate Nitrogen

The ammonia was always the major contributor to the overall nitrogen in the leachate as a result of the decomposition of organic matter containing nitrogen, such as protein and amino acids. The long-term, high-concentration ammonia accumulation was observed in the leachate from reactor R1 as reported by [5–7], and this phenomenon often occurred in the anaerobic bioreactor landfill. As was shown by Fig. 4a, the leachate NH_4^+-N concentrations for reactor R1 started to increase quickly and accumulated to more than 2,000 mg L^{-1} within the first 28 days. After a stabilized period of 42 days, the leachate NH_4^+-N concentrations started to decrease and reached 1,658 mg L^{-1} on day 91. After that, no significant change was found, and the leachate NH_4^+-N concentrations were maintained at approximately 1,400 mg L^{-1}. The results of the present study are similar to those of [2, 8] and clearly showed that there is no mechanism for NH_4^+-N elimination in anaerobic landfills [9]. Nevertheless, the NH_4^+-N curves for reactors R2 and R3 presented a distinct trend, both of which increased slowly at the beginning of the

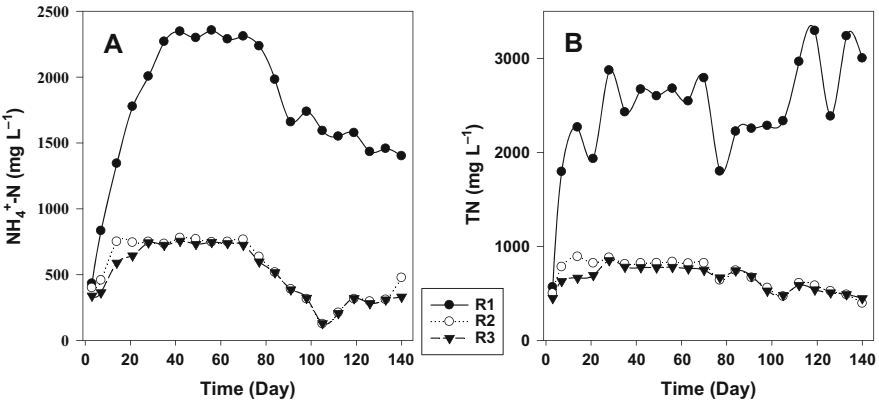

Fig. 4 Time evolutions of NH_4^+-N (**a**) and TN (**b**) in leachate during operation

28 days, and reached maximum values of 750 and 744 mg L^{-1}, respectively. Afterwards, no significant change was found during the succeeding 8 weeks, and the leachate NH_4^+-N concentrations for reactors R2 and R3 started to decrease gradually and the concentrations were determined to be 125–500 mg L^{-1}. The different NH_4^+-N concentration behavior among the two reactors, R1 and R2, might be attributed to the leachate recirculation management strategy, although these two reactors were loaded with the same refuse, which was in accordance with previous research [2]. As aged waste has a smaller particle size and thus a larger surface area, yielding more available reactive sites for sorption, the NH_4^+-N released from reactor R2 was removed by the adsorption of well-decomposed refuse in R3. On the contrary, as younger waste does not have enough potential for sorption, most of the NH_4^+-N generated from reactor D3 accumulated in the leachate. In the later period, the NH_4^+-N concentration in the leachate of reactor R1 decreased, which might have resulted from the formation of free ammonia from ammonium ions due to the increased pH and temperature, which was in accordance with previous research [10].

The TN values were in accordance with the concentration of NH_4^+-N monitored for both reactors (Fig. 4b). The leachate TN concentrations for reactor R1 increased quickly and accumulated to more than 2,871 mg L^{-1} within the first 28 days. After two stabilized periods (more than 70 days), the leachate TN concentrations started to increase again and reached 3,290 mg L^{-1} on day 119. After that, the leachate TN concentrations maintained approximately at 3,200 mg L^{-1} with a little fluctuation on day 126. However, the leachate TN concentrations for reactors R2 and R3 showed a significant trend, which was also in accordance with the change in leachate NH_4^+-N concentration. The leachate TN concentrations for both reactors increased slowly at the beginning of 28 days and reached the maximum values of 881 and 852 mg L^{-1}, respectively. Afterwards, no significant change was found during the succeeding 6 weeks. From day 70, the leachate NH_4^+-N concentrations for reactors R2 and R3 started to decrease gradually and finally stabilized at around 447 and 390 mg L^{-1}. Above all, the combined system of fresh and aged refuse reactor not only had a positive effect on the stabilization of fresh refuse but also on the degradation of leachate.

2.1.4 Summary

After 140 days of digestion, the refuse and leachate in the reactor connected with the aged refuse column reached a strongly degraded and more stable state compared with directly recycled leachate. The key constituents in the leachate, such as COD, NH_4^+-N, and TN, were able to meet the related discharge criteria.

2.2 KW Composting After Source Separation

KW in Hangzhou after source separation shows a special feature. As shown in Fig. 5, the moisture content of separated KW was always higher than 80%. Obviously, it is not feasible to compost before dewatering. The relatively low pH (5.0–6.0) may be caused by the partial AD during the dumping. It indicates that the KW has high biotransformation potential. Based on those basic characteristics of the KW after separation, dewatering should be taken into consideration during composting. Therefore, the cases of water state adjusting coupled with kitchen waste composting are presented.

In order to evaluate the moisture content adjusting effect, the water states were analyzed using a gradient evaporation technique. About 10 g of a finely chopped sample were spread uniformly on a glass tray (90 mm in diameter), and the tray was placed in an electrically heated air blast dryer (GZX-9076; MBE, Shanghai, China). The analysis was performed in stages at 30, 40, 50, 60, 70, 80, 90, 100, and 105°C. A residence time of 1 h was used at each temperature except for 105°C, and the time at 105°C was 2 h. After the residence time had been reached at each temperature stage, the temperature was increased to the next test temperature. The mass of each sample was carefully measured before and after drying at each temperature. The water removed at 30, 40, and 50°C was classed as EW; the water removed at 60 and 70°C was classed as CW; and the water removed at 80, 90, 100, and 105°C was classed as MMLW (Fig. 6). The water removed throughout the whole-gradient evaporation test was used to calculate the moisture content of the sample (Table 1).

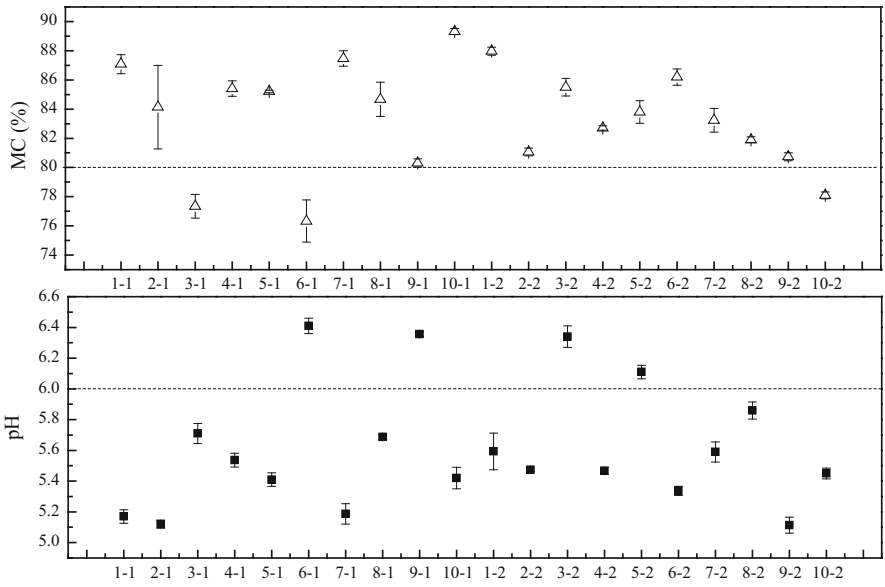

Fig. 5 Characterization of separated KW based on a 10-month survey in Hangzhou

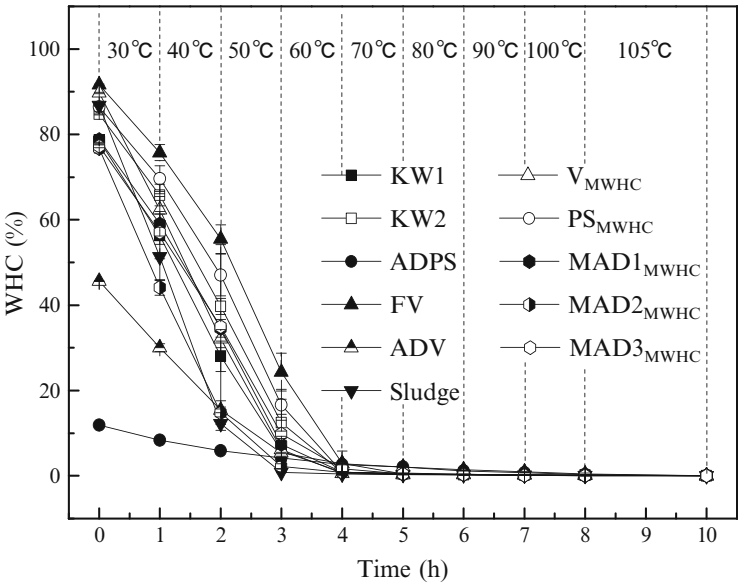

Fig. 6 WHCs of the samples during the gradient temperature test. The WHC at 0 h is the initial WHC of the sample; and the WHCs at 1, 2, 3, 4, 5, 6, 7, 8, and 10 h are the WHCs of the sample after it had been dried at 30, 40, 50, 60, 70, 80, 90, 100, and 105°C, respectively

Table 1 Statistical results for the linear models for each heating stage

	Stage 1 (room temperature, 30, 40, 50°C)		Stage 2 (60, 70°C)		Stage 3 (80, 90, 100, 105°C)	
Sample name	R^2	P	R^2	P	R^2	P
KW1	0.997	0.001	0.536	0.320	0.947	0.003
KW2	0.990	0.003	0.544	0.317	0.931	0.005
ADPS	0.963	0.012	0.870	0.164	0.932	0.005
PS_{MWHC}	0.974	0.009	0.539	0.319	0.972	0.001
FV	0.964	0.012	0.652	0.274	0.993	1.616×10^{-4}
ADV	0.986	0.005	0.824	0.192	0.991	2.231×10^{-4}
V_{MWHC}	0.999	3.850×10^{-4}	0.557	0.312	0.968	0.002
Sludge	0.937	0.021	0.853	0.175	0.991	2.188×10^{-4}
$MC1_{MWHC}$	0.993	0.002	0.608	0.292	0.982	6.487×10^{-4}
$MC2_{MWHC}$	0.951	0.017	0.789	0.211	0.912	0.007
$MC3_{MWHC}$	0.996	0.001	0.691	0.257	0.911	0.007

2.2.1 Using PAM for Water State Adjusting During the Composting

Materials and Methods

The raw material was fresh KW and air-dried garbage. The air-dried garbage was prepared from fresh garbage that was generated in food pretreatment processes, and it was used as a bulking agent for the composting system. All of the fresh KW and garbage was cut into pieces with diameters of 5.0 ± 0.5 cm. The cut fresh garbage was naturally air-dried for about 7 days to allow the excess water to evaporate, and then the air-dried garbage had been stored in an airtight plastic bag before use. The moisture content of the fresh KW and the air-dried garbage was 73.2% and 12.1%, respectively. PAM with a molecular weight of 3.0×10^6 Da was used. High-performance mixed flora, acclimatized and isolated from our previous work [11] and preserved at below −80°C in glycerol, was used as inoculums for the composting experiments. The flora contained microorganisms that could decompose starch, glucose, and protein. Before inoculation, the high-performance mixed flora was activated in a Luria-Bertani culture medium [12]. The concentration of the high-performance mixed flora seed that was used was higher than 1×10^{15} CFU mL^{-1}.

A laboratory-scale reactor with an effective volume of 16 L was developed for this composting trial (Fig. 7). The reactor consisted of an insulated cylindrical vessel, an air pump, a gas rotameter, and a temperature recorder with a thermometer probe. The vessel was made of plastic, and it was surrounded by a layer of rubber insulation board (20 mm thick) and covered with an insulating layer of straw (50 ± 5 mm thick). The thermometer probe was mounted in the center of the

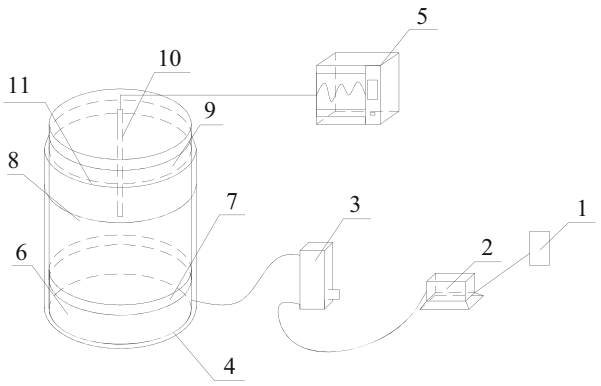

Fig. 7 The composting setup tested [13]

1 Electronic relay
2 Air pump
3 Gas rotameter
4 Reactor
5 Temperature recorder
6 Aeration chamber
7 Rubble layer
8 Reactor chamber
9 Overlay
10 Temperature probe
11 Insulating layer

Table 2 The chemical characteristics of the mixture

Parameter	Value	Parameter	Value
Moisture content (%)	60.30 ± 0.90	NDS (%)	73.75 ± 1.67
C/N	26.55 ± 0.95	Hemicellulose (%)	14.89 ± 1.38
pH	4.92 ± 0.07	Cellulose (%)	6.95 ± 0.74
EC (mS cm^{-1})	1.99 ± 0.12	Lignin (%)	4.08 ± 0.63

composting pile, and the temperature was recorded once every 20 s. An aeration chamber was installed at the bottom of the vessel to maintain aerobic conditions, and the airflow rate was continuously controlled using a gas rotameter.

Four composting treatments, each with an initial moisture content of 60%, were used. The chemical characteristics of the mixture are shown in Table 2. To each system, 1 mL/kg of the high-performance mixed plant inoculum was added to the waste material. PAM was introduced into the four treatments at different times. R1 had 0.1% PAM added before the start of the composting process (day 0). R2 had 0.1% PAM added when composting stabilized in the thermophilic phase (at >50°C) (day 3). R3 had 0.1% PAM added when the moisture content had decreased significantly (day 7), and R4 had no PAM added. All four treatments were performed in a greenhouse (at 29 ± 1°C), the aeration rate in each was 0.8 L min^{-1}, and all four treatments had three replications at the same time.

Results

Temperature and Moisture Content

Temperature variations in all of the treatments are shown in Fig. 8a. The temperature followed a three-phase pattern in all of the treatments, and this pattern had a mesophilic phase, a thermophilic phase, and a curing phase. In the mesophilic phase (days 0–3), R1 had the highest temperature (>50°C), and this suggests that the PAM decreased the number of air-filled pores in R1, and that less heat was removed by the flowing air. In the thermophilic phase, the peak temperature was lower in R1 than in R2 and R3. The lower number of air-filled pores in R1 caused poor oxygen supply and less heat being produced in the composting system.

In the thermophilic phase (days 3–11), the peak temperatures in R1, R2, R3, and R4 were 57.8, 60.2, 63.9, and 57.8°C, respectively. There was a temperature increase in R2 and R3 after the PAM was added, and R2 remained at high moisture content between days 0 and 8 (Fig. 8b). The moisture content of R3 was higher on day 8 than on day 6. PAM can delay the decrease in moisture content, and that maintaining suitable moisture content could increase the level of microbial activity. Correspondingly, it also causes the accumulation of heat and the rise in temperature in the composting system.

The moisture content for all of the treatments throughout the 16 days experiments is shown in Fig. 8b. The moisture content in R3 and R4 had decreased

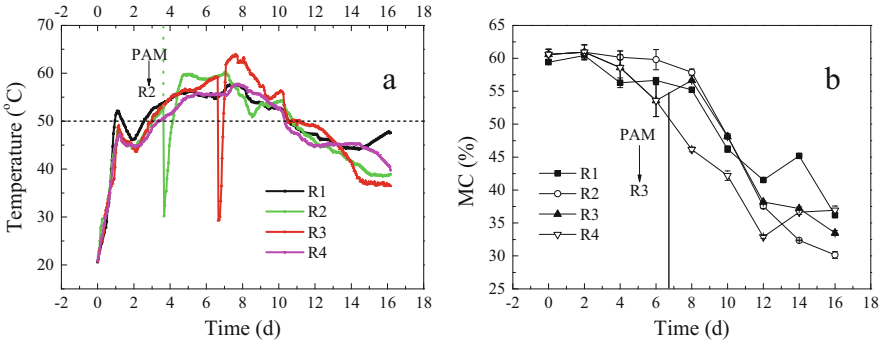

Fig. 8 Temperature (**a**) and moisture content (**b**) in the KW composting process

significantly by day 6, and the moisture content in these treatments was significantly lower than the moisture content in R1 and R2 on day 6, so 0.1% PAM was added to R3 to suppress the decrease in moisture content on that day. The changes in the moisture content in all of the treatments showed that PAM could improve the water holding capacity of the composting system.

As Fig. 9 shows, there were no visible differences in the MMLW values among the treatments, and the percentage of MMLW in all of the treatments fluctuated within a small range (3.9 ± 1.4%). This indicates that 0.1% PAM did not have any effect on the MMLW, and that the MMLW had no effect on variations in the moisture content in the composting systems. Changes in the water states mainly occurred in the EW and CW. The changes in the water states in all of the treatments followed similar trends, the percentage of EW followed an upward trend and the percentage of CW followed a downward trend, although the rate of change in the water states was different in each composting system (Fig. 9). For most of the time, the percentage of CW was higher in R1 and R2 than in R4 (Fig. 9a, b), and meanwhile the moisture content was higher in R1 and R2 than in R4 (Fig. 8b), which suggests that PAM improved the capillary force and retarded the processes that changed CW into EW in the composting systems and restrained the decrease in moisture content. There were no significant differences in the percentage of CW values in R3 and R4 (Fig. 9c), which may have been caused by the moisture content in R3 being relatively low (53.6 ± 2.6%) when the PAM was added to R3, meaning that less water could combine with the PAM in R3 than in R1 and R2. This indicates that the PAM should be added to the composting system when the moisture content in the composting system has not decreased significantly. The water states in R1 fluctuated between days 0 and 8, suggesting that the water had not been completely dispersed in the composting system when the PAM was added to R1.

pH and Electrical Conductivity

The changes in the pH found in each of the treatments are shown in Fig. 10a, and it can be seen that all of the treatments showed similar trends. At the beginning of the

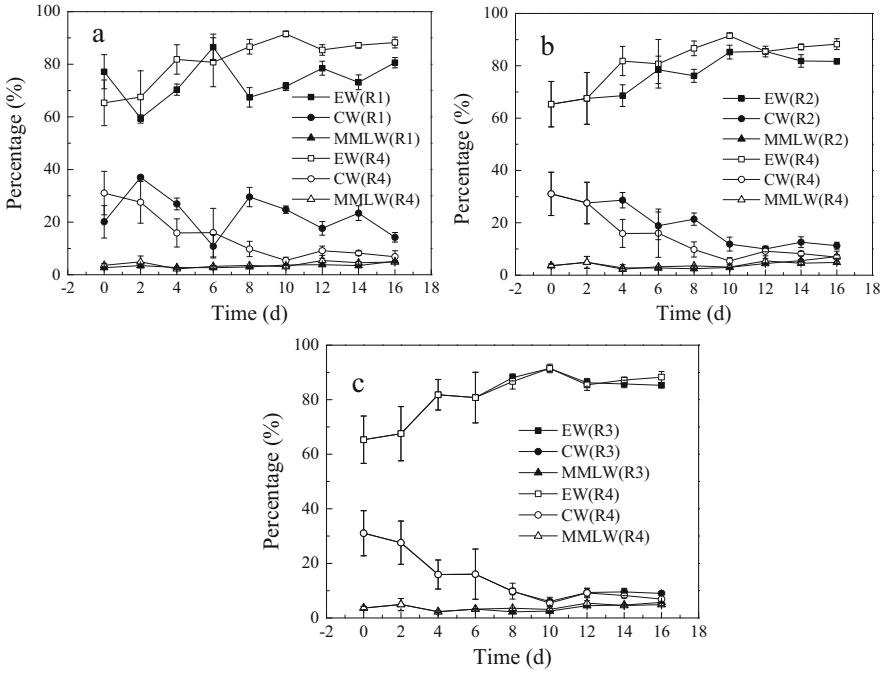

Fig. 9 Variation of water states (EW, CW, and MMLW) in the composting process

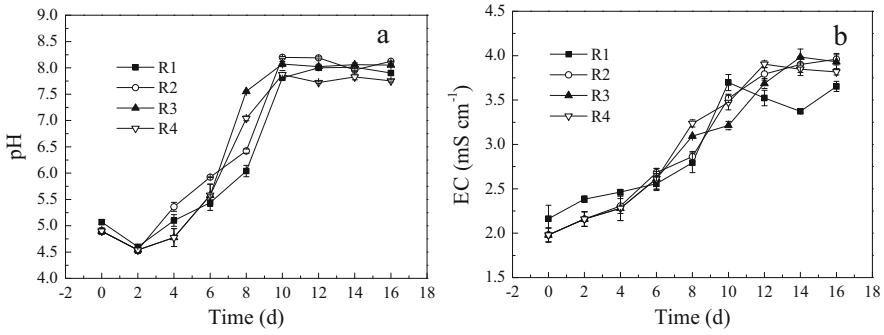

Fig. 10 pH (**a**) and EC (**b**) in the kitchen waste composting process

composting process, the kitchen waste was hydrolyzed very rapidly, and on day 2, the pH in all of the treatments had reached a minimum value (4.6 ± 0.1), coinciding with a downward trend in the temperature in the composting systems. On day 8, the pH values were lower in R1 and R2 than in R3 and R4, and this may have been caused by the moisture content in R1 and R2 still being high (59.8 ± 0.4%) when the PAM was added to them, so more water was absorbed

by the PAM. The PAM in those cases may have acted as a bridge between the kitchen waste particles [14], making the KW particles agglomerate together, causing there to be less air-filled pores in R1 and R2 than in R3 and R4, and a higher percentage of CW values in R1 and R2 than in R3 and R4. This indicated that the mass transfer of water and air was inhibited in R1 and R2, and meanwhile the decomposition of organic acids was inhibited in R1 and R2. Between days 10 and 16, the pH values of the samples from the different treatments stabilized at about 8 without significant differences between treatments. The high pH may be due to the mineralization of organic nitrogen to ammonia nitrogen [15].

The variations in the EC in all of the treatments are shown in Fig. 10b, and it can be seen that the EC showed an increasing trend in all of the experiments. This could have been caused by the concentrating effect of the loss of water and the release of mineral salts and ammonium ions caused by the decomposition of organic matter [16–18]. After day 10, the EC was lower in R1 than in the other treatments, which might have been caused by the moisture content being higher in R1 than in the other treatments, leading to the very poor decomposition of organic matter in R1.

Effects of PAM on the Biodegradation Process

The alkali extractable organic-C is produced and the humic acid-like organic-C increases during composting, so the percentage of humic acids can be used as an index of compost humification [19]. As Table 3 shows, the significant differences in the percentage of humic acid values in each of the treatments could be seen on day 16, and R2 was found to be the most mature, and R3 was also more mature than R4. This indicates that 0.1% PAM had a positive effect on the maturity achieved in the composting system, and this was because the PAM delayed the decrease in the percentage of CW and moisture content. This effect was not apparent in R1, and this was due to the water not being completely dispersed in the materials when PAM was added. This indicates that the time that PAM is added is a key parameter and that this time should be determined by the changes in the water states in the composting system, in that the water should be completely dispersed and the water states should show a relatively stable trend and that the percentage of CW shows a downward trend.

The biochemical composition of the kitchen waste was determined by a crude fiber analysis and expressed as the percentage of total solids at each sampling point. The biochemical fractions of the biowaste were divided into two fractions, the NDS and NDF. The NDF can be further subdivided into three major fractions: hemicellulose, cellulose, and lignin [20]. As Fig. 11 shows, the NDS was the predominant organic matter component in the composting systems containing kitchen waste, and

Table 3 Percentage of humic acids of the initial and final compost (%)

	R1	R2	R3	R4
Initial	9.63 ± 2.24			
Final	20.47 ± 1.86	25.53 ± 1.81	22.82 ± 0.69	21.36 ± 0.39

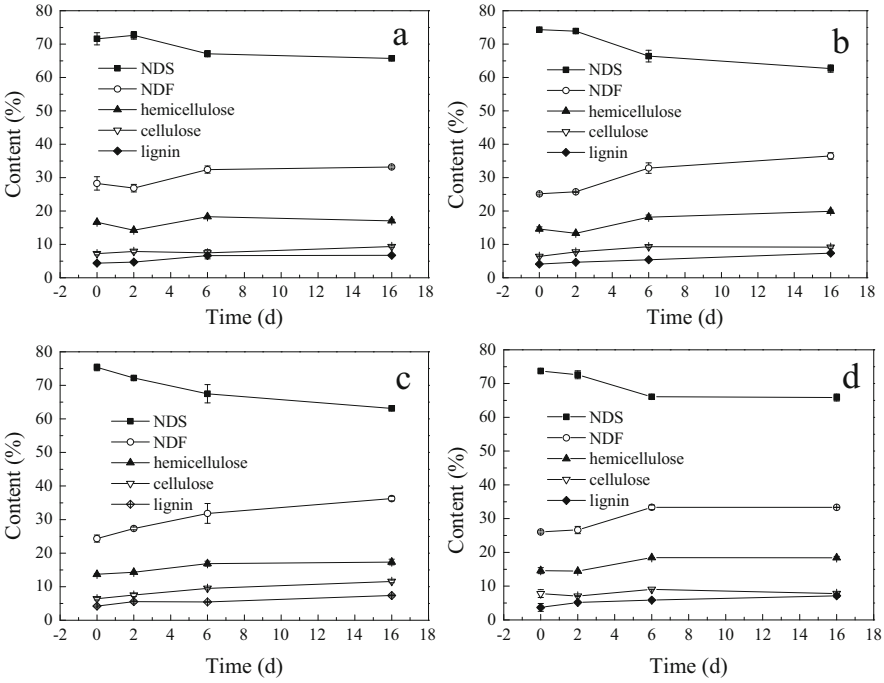

Fig. 11 Biochemical fractions (NDS, NDF, hemicellulose, cellulose, and lignin) in the KW composting process (**a**, **b**, **c**, **d** represented R1, R2, R3 and R4, respectively)

the main NDF component was hemicellulose. In all of the experiments, NDS decreased strongly within the first 6 days of composting, during which time the mineralization of easily biodegradable organic matter by the microorganisms dominated the decomposition of organic matter [21].

The better percentage of humic acid performances in R2 and R3 indicated that more lignin had been transformed into humic acids in these experiments, and although an increase in the lignin content was observed in R2 and R3, a decrease in NDS was also observed in R2 and R3. This suggests that the actual NDS degradation rates were higher in R2 and R3 than in R1 and R4.

The variations that were seen in every biochemical fraction suggest that adding PAM after the water had been completely dispersed in the material promoted the degradation of NDS, as well as the humification of the organic matter.

Summary

PAM can significantly enhance the capillary force and delay the decrease in moisture content and CW during aerobic decomposition, and improve the composting process. However, the effects of PAM on the humification degree of the product and the degradation of biochemical fractions are also affected by the

time that the PAM is added. To maximize its performance, add PAM to the composting of kitchen waste when the water has been completely dispersed and the moisture content has not decreased significantly. The initial stage of the thermophilic phase is the optimal time to add PAM to the composting of KW.

2.3 *Kitchen Waste Co-digestion with Fruit and Vegetable Waste*

FVW is another kind of organic solid waste that mainly comes from food markets and households. FVW comprise 25–30% of the total yield of fruits and vegetables. Reports have indicated that almost 100 million tons of FVW are discarded every year in China [22]. Compared with KW, FVW has low salinity and fat content. Therefore, we suggest that the co-digestion of FVW and KW by AD may be a good choice to treat them. Co-digestion may also promote the co-disposal of two kinds of special organic solid waste. This case aims to develop a solid waste co-disposal method that is economically and technically feasible.

2.3.1 Materials and Methods

The KW and FVW were cut into pieces with a particle size lower than 5 mm using a multifunctional food mixer (Philip I-IR-2860, Netherlands). The inoculated sludge of the two-phase AD was a type of salinity-tolerant anaerobic sludge with the highest tolerable salinity concentration of 3% after 126 days of acclimatization [22]. The characteristics of KW, FVW, and inoculated sludge are shown in Table 4.

The two-phase AD consists of APR and MPR. The APR was made out of a 2.5 L glass bottle. The MPR was an upflow anaerobic sludge bed with a diameter, height, and active volume of 56 mm, 500 mm, and 1.2 L, respectively. The specific pieces of equipment are shown in Fig. 12.

Sixteen APRs and four MPRs were set. Each MPR matched four APRs that had similar proportions of KW and FVW. All of the reactors run in a greenhouse (30–33°C). Detailed information on the material composition within the mixtures in the APR can be found in Table 5. Every APR was inoculated with KW, FVW, and acclimated sludge. The total matrix volume was about 1.5 L, and the sludge concentration was 20 g L^{-1}. According to the pre-experimental results, the COD of all APR had a significant drop on day 9. To improve the sludge adaptability, all of

Table 4 Characteristics of experiment materials (wet weight)

	TS (%)	Salinity (%)	Fat content (%)	pH
KW	10.12 ± 0.27	0.20 ± 0.02	0.43 ± 0.08	6.53 ± 0.01
FVW	10.06 ± 0.07	0.65 ± 0.03	0.22 ± 0.04	6.21 ± 0.02
Inoculated sludge	14.81 ± 0.24	2.94 ± 0.13	/	7.39 ± 0.05

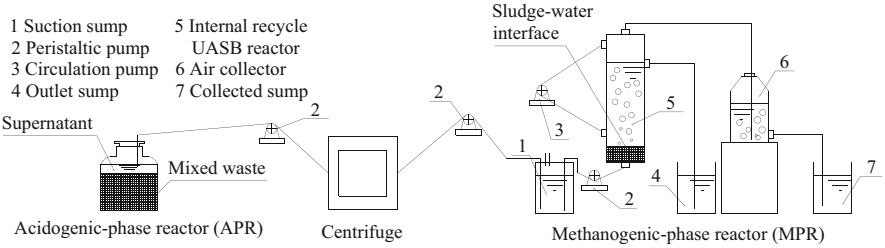

Fig. 12 The reactor of two-phase AD [11]

Table 5 The material composition within the mixtures of the APR

APR	A	B	C	D
Total mass (g)	1,551.60	1,586.25	1,590.90	1,655.55
KW (g)	375.00	750.00	1,125.00	1,500.00
FVW (g)	1,125.00	750.00	375.00	0
Inoculated sludge (g)	30.00	30.00	30.00	30.00
Salinity (g)	11.25	22.50	33.75	45.00
Fat content (g)	22.50	45.00	67.50	90.00

Every set of devices (A, B, C, D) had four APRs, each one of them operated at different HRTs of 5, 10, 15, and 20 days, respectively. The corresponding MPR was named a, b, c, and d, respectively

the APRs were pre-run for 10 days without continuous feedstock, sampling and determination, as in the following trials. To optimize the HRTs of A, B, C, and D, all of the APRs were first run for 24 days with the set HRT, and the pH, VS, TS, VFA, and COD of all the supernatants were determined. After optimization, all of the APRs were set to run with their corresponding optimal HRT. When the operation of all the APRs was stable, all of the MPRs were started.

In each MPR, the initial sludge concentration was set as 50 g L^{-1}. During the running process, the supernatant from each group of four APRs was centrifuged daily and merged as the influent of the MPR. Considering the low pH shock, the pH of the influent was first adjusted to 5.5–6.0. The influent was then pumped into the MPR through a peristaltic pump. The influent water flow rate was initially set as 12–13 mL h^{-1}. Subsequently, the water flow rate was improved to shorten the HRT and to enhance the load of MPR step by step according to its running status. To keep raising the flow rate and buffer the high COD concentration in the MPR, the internal reflux was continuously carried using a peristaltic pump with a flow rate of 2–2.5 mL min^{-1}.

2.3.2 Results

Effect of HRT on APR

The pH of the APRs with different KW proportions varied greatly as the HRT. Figure 13 shows the pH of the APR with 25% KW after stabilization for 18 days, whereas the others only required 12 days. The main reason for the difference was that the FVW proportion of APR with 25% KW (75% FVW) was significantly higher than that of the others (50%, 25%, and 0% FVW, respectively) ($p < 0.05$). The KW included 70% rice in the total wet weight, and the rice is full of carbohydrate, and the carbohydrate is more easily degradable than hemicellulose, cellulose, and lignin. So, the hydrolysis efficiency of KW was higher than that of FVW. And the pH of all APRs was lower than 4.0, and the reason for this performance was that high organic content could improve the degree of acidification.

Specifically, in APR A (25% KW), the change in pH of each APR had a wider range, and the final pH of APR A_{15} (HRT = 15 days) was higher than the other APRs ($pH(A_{15}) = 3.88$, $pH(A_5,A_{10},A_{20}) = 3.21 \pm 0.05$); the high pH means low VFA accumulation [23], so this result suggested that 15 days is not an appropriate HRT for APR A. At the preliminary stage (0–6 days), the change in pH of APR A may have been caused by the 25% KW having a low salinity and fat content, and the microbes hadn't been inhibited by this salinity and fat content. The pH of all APR A

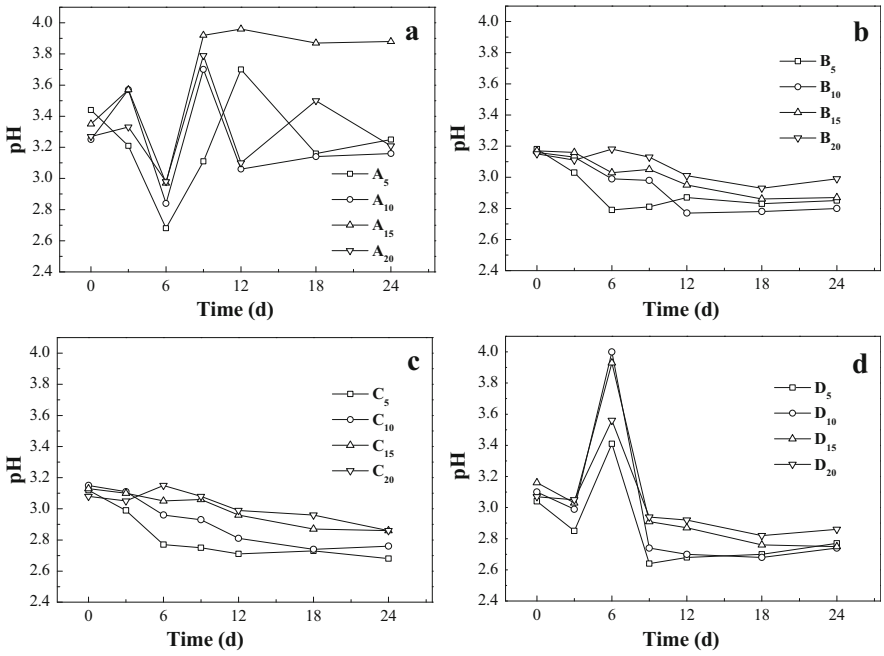

Fig. 13 The change in pH of each APR at different HRT

was below 3.0 on day 6, meaning that the degree of acidification was great. In APR B and APR C, the changes in pH had a lesser range. All of the APRs of the B and C series (with an HRT of 5, 10, 15, and 20 days, respectively) exhibited a similar trend. This trend suggested that the APR of 50 and 75% KW could offer appropriate conditions with moderate salinity and fat concentration. For APR D, there was a drastic change in the pH at the beginning of the 9th day, and there was a sharp rise followed by a slower decline, which ended up with a sharp decline. At the preliminary stage (day 0–6th), the acidification was inhibited by low microbial activity. Then the microbe adjusted to the above feeding method, the microbial activity was renewed, and the pH declined again. The trend also indicated that the adaptation time of the sludge should be more than 10 days in APR D, and this may be caused by the high salinity and fat content.

In the acidogenic stage of AD, the acidogenic bacteria consumed organic matter, which caused a corresponding change in the TS and VS of the matrix. Therefore, the ratio of VS/TS could indirectly characterize the degradation degree of the material. The changes in VS/TS (%) of the APR at different HRTs were shown in Table 6. In all of the APRs with 25% KW, the degradation rate of the APRs with HRTs of 5 and 10 days were higher than those with HRTs of 15 and 20 days. This result suggested that 5–10 days may be the optimal HRT of APR with 25% KW. In all of the APR B with 50% KW, if the HRTs were 5, 15, and 20 days, the degradation rate would be higher than the HRT of 10 days. In all of APR C and D, the degradation rates of APR C_{15} and D_{20} were higher than those of the others. Thus, APR C_{15} and D_{20} can be used as optimal APRs.

Table 6 The daily discharge and feedstock of each APR at different HRT

APR	HRT (days)	Discharge (g)	Feedstock			
			KW (g)	FVW (g)	Salinity (g)	Fat content (g)
A	5	300.00	75.00	225.00	2.25	4.50
	10	150.00	37.50	112.50	1.13	2.25
	15	100.00	25.00	75.00	0.75	1.50
	20	75.00	18.75	56.25	0.56	1.13
B	5	300.00	150.00	150.00	4.50	9.00
	10	150.00	75.00	75.00	2.25	4.50
	15	100.00	50.00	50.00	1.50	3.00
	20	75.00	37.50	37.50	1.13	2.25
C	5	300.00	225.00	75.00	6.75	13.50
	10	150.00	112.50	37.50	3.38	6.75
	15	100.00	75.00	25.00	2.25	4.50
	20	75.00	56.25	18.75	1.69	3.38
D	5	300.00	300.00	0.00	9.00	18.00
	10	150.00	150.00	0.00	4.50	9.00
	15	100.00	100.00	0.00	3.00	6.00
	20	75.00	75.00	0.00	2.25	4.50

Table 7 The change in VS/TS (%) of each APR at different HRT

Time (days)	0	3	6	9	12	18	24
A_5	37.70	33.33	32.65	28.57	26.66	25.60	25.59
A_{10}	36.36	33.85	34.62	28.07	24.49	24.19	23.63
A_{15}	37.29	34.29	35.35	32.31	31.58	29.24	29.19
A_{20}	39.66	38.81	36.84	33.33	32.73	30.30	28.87
B_5	36.75	33.96	34.04	34.21	38.24	30.72	28.26
B_{10}	34.71	35.48	32.79	31.58	33.33	29.71	28.16
B_{15}	37.88	35.29	33.67	31.82	32.79	31.34	30.40
B_{20}	38.81	38.24	33.33	33.80	33.33	31.46	31.31
C_5	37.14	41.79	34.04	36.00	36.23	36.73	33.05
C_{10}	38.14	37.04	33.33	32.69	35.51	34.55	34.22
C_{15}	38.71	37.18	37.29	35.09	35.00	33.90	34.00
C_{20}	40.00	37.66	36.25	36.17	35.16	37.50	37.49
D_5	34.95	39.22	32.36	38.18	29.69	24.72	29.51
D_{10}	37.22	41.82	34.79	37.50	34.52	31.00	31.06
D_{15}	41.10	40.74	38.96	38.98	37.21	36.17	35.30
D_{20}	40.00	40.83	38.55	39.66	35.71	33.56	33.17

In the acidogenic stage of AD, the ratio of VFA/CODs can indirectly characterize the acidification degree of the materials. The changes in VFA/CODs of APR at different HRTs are shown in Table 7. There was a decreasing trend in the VFA/CODs with the increase in the proportion of KW. These results can be attributed to the increase in concentrations of salinity and fat in the matrix. The high concentrations of salinity and fat can seriously inhibit the microbial activity, while the acidification degree decreased correspondingly.

The results further indicated that the APRs with KW of 25%, 50%, 75%, and 100% had the highest acidification degree at 85.66%, 74.11%, 70.11%, and 56.63% when their HRTs were 10, 15, 15, and 20 days, respectively.

Performance of MPR

The changes in pH and alkalinity of the MPR effluent are shown in Fig. 14. These data indicated that the process consisted of two periods before the HRT of MPR was changed. The first was the adjustment phase (day 0–8), and the second was the stationary phase (days 10–15). The effluent pH and alkalinity rose with the fluctuations in the first 8 days and then became relatively steady from day 10 to 15. After day 15, the MPR HRT was adjusted from 4 to 3 days. The change in pH and alkalinity showed a similar trend in that all of the MPRs had a sudden decrease on day 16. In all of the MPRs, the pH and alkalinity gradually increased and then stabilized within a specific range in the former 15 days (HRT = 4 days).

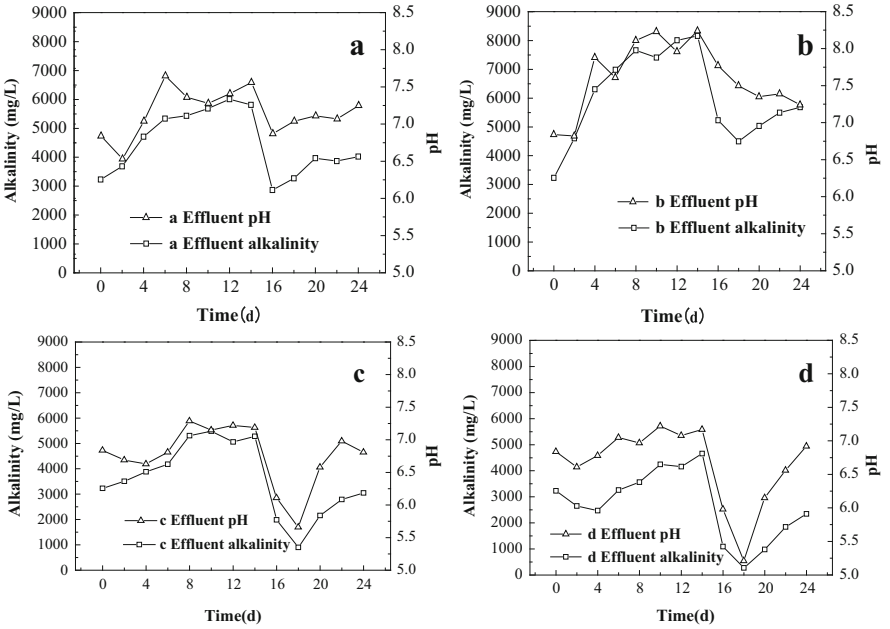

Fig. 14 The change in pH value and alkalinity in each MPR

In MPRs a and b, the pH and alkalinity decreased after the increase in the organic load, but recovered rapidly with the extension of the fermentation time. After day 20, the pH and alkalinity stayed at a relatively stable level, indicating that the optimal HRT of MPRs a and b was 3 days, but the final alkalinity was slightly lower than that of 4 days. The results showed that alkalinity gradually and consistently increased with the extension of HRT.

In MPRs c and d, pH and alkalinity decreased after the enhancement of the organic load, but did not recover as in MPRs a and b. The main reason could be the higher concentrations of salinity and fat of the influent of MPRs c and d. Therefore, the impact of adjusting HRT was greater in MPRs c and d. To avoid further acidification, the HRT was adjusted back to 4 days on day 18. Subsequently, the pH and alkalinity returned to their former levels, indicating that the optimal HRT of MPRs c and d was 4 days. Thus, the MPR with a higher KW proportion should run in a short HRT.

The changes in daily methane production are shown in Fig. 15. The figure revealed that all of the trends were similar to the changes in pH and alkalinity and that the optimal tested HRTs of MPRs a, b, c, and d were 3, 3, 4, and 4 days, respectively. Moreover, the daily methane production of MPR b was higher than that of the others after becoming stable. This difference could be because MPR b could provide more sufficient nutrients for methanogens than MPR a. At the same time, MPR b reduced the negative impact caused by high concentrations of salinity and fat compared with MPRs c and d.

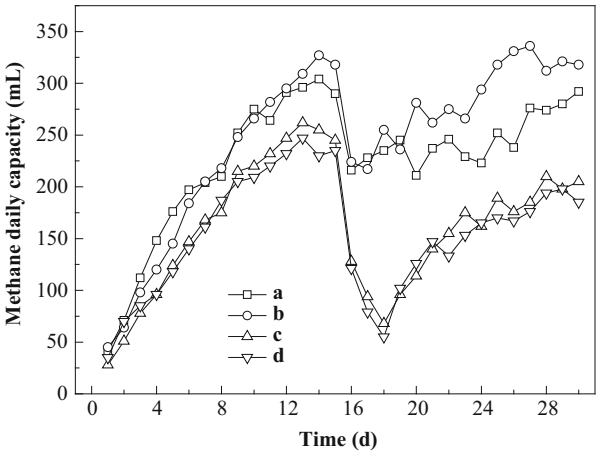

Fig. 15 The change in daily methane production in each MPR

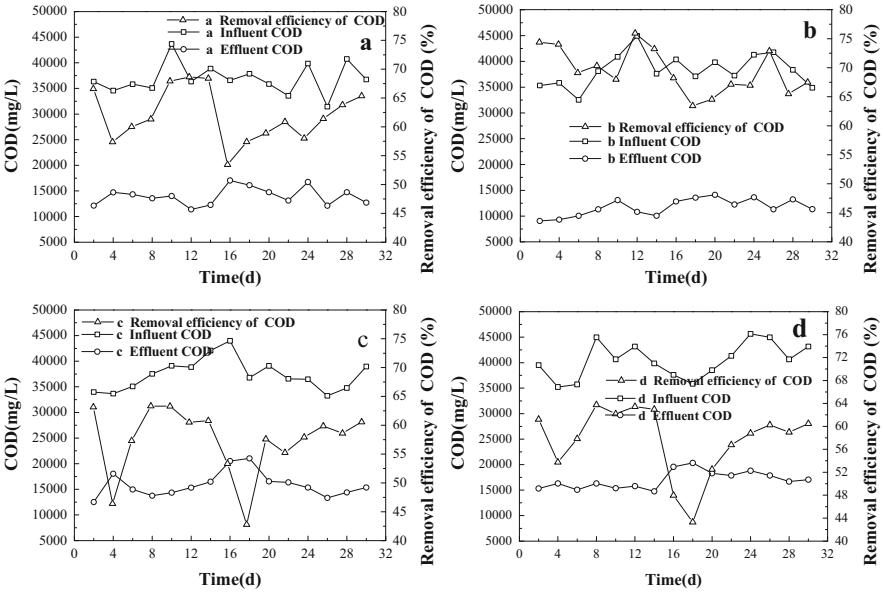

Fig. 16 The change in COD in each MPR

Figure 16 shows that the influent COD was high and changeable. In day 2, all of the MPRs had a higher COD removal efficiency. In comparison, in MPRs a, c, and d on day 4 (MPR b on day 6), the COD removal efficiency followed a sharp downward trend, and then showed an upward trend from days 5 to 10 (MPR b on days 7–12), finally remained relatively stable from days 10 to 14 (MPR b had a

slight downward trend on day 14). This result could be due to the adsorption of sludge, which caused the COD removal efficiency to remain at a high level in the beginning. Thus, when the COD removal efficiency decreased later, it could have been caused by the desorption of sludge and microorganisms that cannot adapt fully to the environment. As the reaction proceeded, the adaptability of the methane bacteria was enhanced and then the methane production increased, which also resulted in the gradual rise in the COD removal efficiency.

After running for 15 days, the HRTs were changed from 4 to 3 days in all of the reactors. The trends of COD removal efficiency were similar to the changes in pH value, alkalinity, and methane production. After the HRT was shortened, the COD removal efficiency of MPR b did not exhibit a significant downward trend compared with MPRs a, c, and d ($p > 0.05$). The COD removal efficiency of MPRs c and d was lower than that of MPRs a and b in the stationary phase, and the COD removal efficiency of MPRs c and d decreased rapidly. These findings indicated that the methanogenus did not resume activity as MPRs a or b. Thus, the HRT of MPRs c and d was restored to the original 4 days, which caused the COD of the effluent to slowly decline and the removal rate to gradually increase. The higher load of salinity and fat concentration had a negative effect on the microbial activity because the KW proportion was higher in MPRs c and d than in the others.

The results of the COD removal efficiency showed that the optimal HRT of MPRs a and b was 3 days, whereas that of MPRs c and d was 4 days. The COD removal efficiency of MPR b was higher than that of the others. Thus, MPR b exhibited a better performance with the change of HRT.

As shown in Fig. 17, the VFA of the influent was high and changeable, with a range of 8,000–12,000 mg L^{-1}. The VFA performance indicated a similar trend as the abovementioned parameters.

In MPRs a and b, the VFA removal efficiency reached more than 90% in the stationary phase (days 10–15). However, after the HRT was changed from 4 to 3 days, the concentration of the effluent VFA rose and the VFA removal rate dropped to below 80% (days 15–20) in MPR a. In comparison, in MPR b, the change in the effluent VFA was not significant ($p > 0.05$), and the removal efficiency remained above 85%.

In MPRs c and d, after the HRT was changed from 4 to 3 days, the VFA removal efficiency rapidly dropped and did not return to its original rate (days 15–18). Thus, the HRT was changed to the original 4 days and the VFA removal efficiency returned to 85%.

The results showed that the optimal HRT of MPRs a and b was 3 days, and the optimal HRT of MPRs c and d was 4 days. The VFA removal efficiency of MPRs a and b was higher than that of the others, and MPR b had a better performance with the change of HRT.

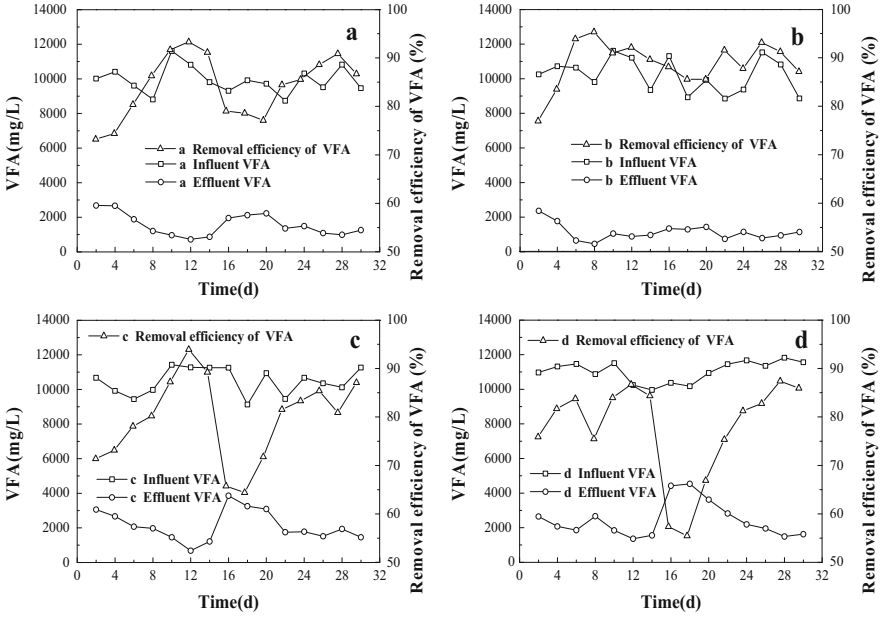

Fig. 17 The change in VFA in each MPR

2.3.3 Summary

The addition of FVW can reduce the HRT and lead to a higher degree of acidification. 25% FVW was better than the others in APR. In MPR, the optimal HRTs of 25 and 50% were 3 days, and the optimal HRTs of 75 and 100% were 4 days. The two-phase AD system with 50% KW not only can dispose more KW than the two-phase AD system with 25% KW but also have better stability in MPR. The 50% KW is the best ratio in this two-phase AD system.

3 Conclusion

MSW digestion without separation is a possible means of refuse disposal. The refuse and leachate in the reactor connected with the aged refuse column reached a strongly degraded and more stable state compared with directly recycled leachate. The key constituents in the leachate, such as COD, NH_4^+-N, and TN, could meet the related discharge criteria. However, the stabilized refuse needs further disposal.

KW composting after source separation is a better choice. However, the high water content is the key issue that needs attention. The percentage of CW decreases while the percentage of EW increases as the composting progresses. The percentage of EW correlated linearly well with dissolved organic carbon, EC, pH, and C/N ratio and is affected by hemicellulose and cellulose. PAM can significantly enhance

the capillary force and delay the decrease in moisture content and CW during aerobic decomposition and improve the composting process.

KW co-digestion with FVW has high application potential. The addition of FVW can reduce the HRT and lead to a higher degree of acidification. Twenty five percent FVW was better than the others in APR. In MPR, the optimal HRT of 25 and 50% was 3 days, and the optimal HRT of 75 and 100% was 4 days. The two-phase AD system with 50% KW not only can dispose of more KW than the two-phase AD system with 25% KW but also have the better stability in MPR. Therefore, the results suggested that the 50% KW is the best ratio in this two-phase AD system.

References

1. World Bank (2012) What a waste: a global review of solid waste management. Urban Development and Local Government Unit, The World Bank, Washington, DC
2. Huo SL, Xi BD, Yu HC, Fan SL, Su J, Liu HL (2008) In situ simultaneous organics and nitrogen removal from recycled landfill leachate using an anaerobic-aerobic process. Bioresour Technol 99:6456–6463
3. Borglin SE, Hazen TC, Oldenburg CM, Zawislanski PT (2004) Comparison of aerobic and anaerobic biotreatment of municipal solid waste. J Air Waste Manage Assoc 54:815–822
4. Nguyen PHL, Kuruparan P, Visvanathan C (2007) Anaerobic digestion of municipal solid waste as a treatment prior to landfill. Bioresour Technol 98:380–387
5. Long Y, Guo QW, Fang CR, Zhu YM, Shen DS (2008) In situ nitrogen removal in phase-separate bioreactor landfill. Bioresour Technol 99:5352–5361
6. He R, Shen DS, Wang JQ, He YH, Zhu YM (2005) Biological degradation of MSW in a methanogenic reactor using treated leachate recirculation. Process Biochem 40:3660–3666
7. Wang Q, Matsufuji Y, Dong L, Huang QF, Hirano F, Tanaka A (2006) Research on leachate recirculation from different types of landfills. Waste Manag 26:815–824
8. Bilgili MS, Demir A, Ozkaya B (2007) Influence of leachate recirculation on aerobic and anaerobic decomposition of solid wastes. J Hazard Mater 143:177–183
9. Vigneron V, Ponthieu M, Barina G, Audic JM, Duquennoi C, Mazeas L, Bernet N, Bouchez T (2007) Nitrate and nitrite injection during municipal solid waste anaerobic biodegradation. Waste Manag 27:778–791
10. Nikolaou A, Giannis A, Gidarakos E (2010) Comparative studies of aerobic and anaerobic treatment of MSW organic fraction in landfill bioreactors. Environ Technol 31:1381–1389
11. Yang YQ, Shen DS, Li N, Xu D, Long YY, Lu XY (2013) Co-digestion of kitchen waste and fruit–vegetable waste by two-phase anaerobic digestion. Environ Sci Pollut Res 20:2162–2171
12. Miller JH (1992) A short course in bacterial genetics: a laboratory manual and handbook for E. coli and related bacteria. Cold Spring Harbor Laboratory Press, Cold Spring Harbor, pp. 24.5–24.6
13. Shen DS, Yang YQ, Huang HL, Hu LF, Long YY (2015) Water state changes during the composting of kitchen waste. Waste Manag 38:381–387
14. Ben-Hur M (1994) Runoff, erosion, and polymer application in moving-sprinkler irrigation. Soil Sci 158:283–290
15. Venglovsky J, Sasakova N, Vargova M, Pacajova Z, Placha I, Petrovsky M, Harichova D (2005) Evolution of temperature and chemical parameters during composting of the pig slurry solid fraction amended with natural zeolite. Bioresour Technol 96:181–189

16. Maeda KK, Hanajima D, Morioka RK, Osada TKS (2010) Characterization and spatial distribution of bacterial communities within passively aerated cattle manure composting piles. Bioresour Technol 101:9631–9637
17. Nair J, Okamitsu K (2010) Microbial inoculants for small scale composting of putrescible kitchen wastes. Waste Manag 30:977–982
18. Said-Pullicino D, Erriquens FG, Gigliotti G (2007) Changes in the chemical characteristics of water-extractable organic matter during composting and their influence on compost stability and maturity. Bioresour Technol 98:1822–1831
19. Iglesias-Jiménez E, Pérez-García V (1992) Composting of domestic refuse and sewage sludge. II. Evolution of carbon and some "humification" indexes. Resour Conserv Recycl 6:243–257
20. Francou C, Linères M, Derenne S, Villio-Poitrenaud ML, Houot S (2008) Influence of green waste, biowaste and paper–cardboard initial ratios on organic matter transformations during composting. Bioresour Technol 99:8926–8934
21. Pichler M, Kögel-Knaber I (2000) Chemolytic analysis of organic matter during aerobic and anaerobic treatment of municipal solid waste. J Environ Qual 29:1337–1344
22. Xu D (2011) Investigation of food wastes and optimization in anaerobic fermentation process. Dissertation of master's degree, Zhejiang Gongshang University, Zhejiang (in Chinese)
23. Han SK, Shin HS (2004) Biohydrogen production by anaerobic fermentation of food waste. Int J Hydrog Energy 29:569–577